

Supplementary Information
Large Band-edge Photocurrent Peak in Thick Methylammonium Lead Iodide
Photosensors with Symmetric Metal Electrodes

Péter Hantz^{||}*, Ferenc Sarlós⁺, István Jalsovszky[§], and Balázs Plesz[⊥]

^{||} University of Pécs, Medical School, Department of Laboratory Medicine, H-7624 Pécs, Ifjúság útja 13, Hungary,

⁺ Biological Research Centre of the Hungarian Academy of Sciences, Institute of Biophysics, H-6726 Szeged, Temesvári krt. 62, Hungary

[§] Eötvös Loránd University, Institute of Chemistry, Department of Organic Chemistry, H-1117 Budapest, Pázmány Péter sétány 1/A, Hungary

[⊥] Budapest University of Technology and Economics, Department of Electron Devices, H-1117 Budapest, Magyar Tudósok körútja 2, Hungary

* Corresponding Author

Péter HANTZ

hantz@general.elte.hu

Some details of the Methods

Sample preparation

If stored for a longer period of time, I_2 , a dissolved oxidation product, might accumulate in the HI solution. This product should be reduced by boiling the solution for a couple of minutes at 127 °C with red phosphorous (1 g to 100 mL solution). After this, the mixture is distilled over the red phosphorous. (Alternatively, HI solution including 1.5 wt.% H_3PO_2 can also be used, where the hypophosphorous acid prevents HI from oxidation).

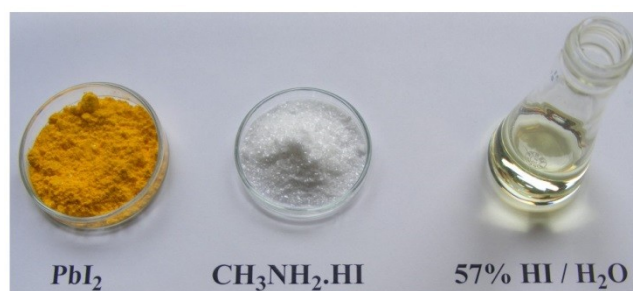


Figure S1. The reagents: 4.61 g PbI_2 (0.01M), CH_3NH_3I 1.59g (0.01M), and 57 wt % HI solution (9 mL).

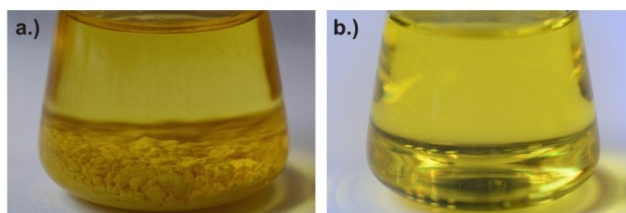


Figure S2. PbI_2 added to the HI solution, before and after heating to about $100\text{ }^\circ\text{C}$

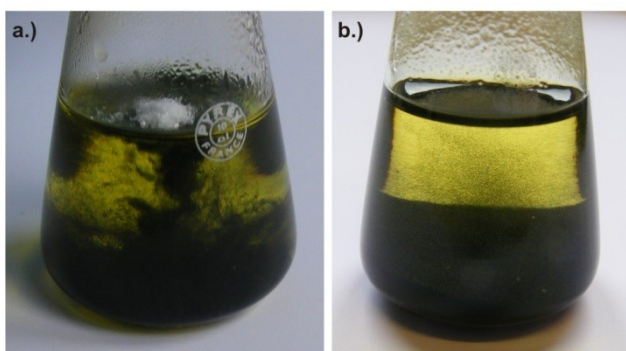


Figure S3. Adding $\text{CH}_3\text{NH}_3\text{I}$ to the PbI_2 dissolved in the HI solution. (a.) shows how the white $\text{CH}_3\text{NH}_3\text{I}$ falls on the surface of the liquid, and yields black MAPbI_3 . (b.) shows the same vessel a few seconds later.

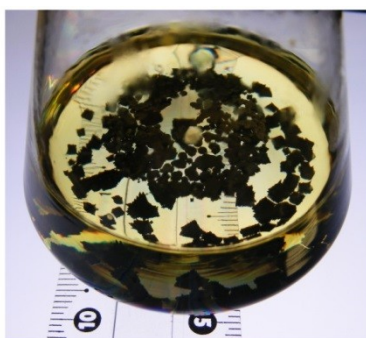


Figure S4. MAPbI_3 crystals in the solution from figure S3 after heating the solution to $100\text{ }^\circ\text{C}$, adding excess HI to it, and cooling it to room temperature.

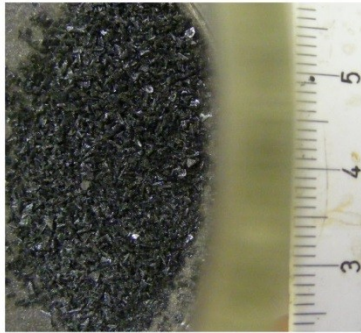
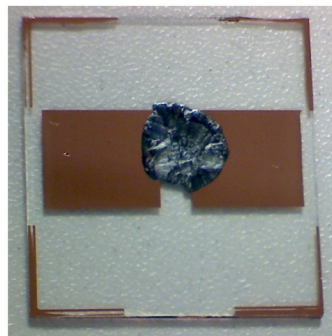
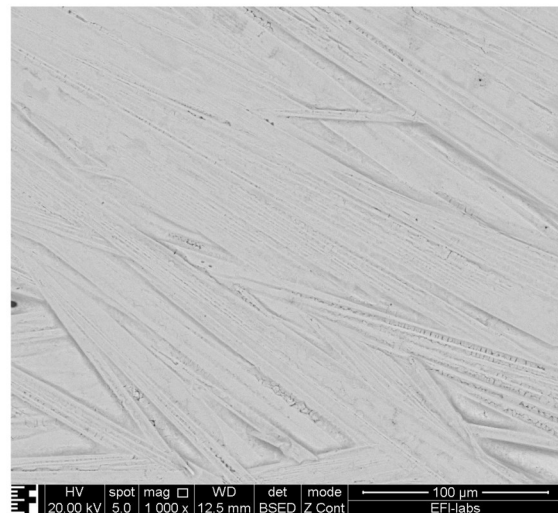
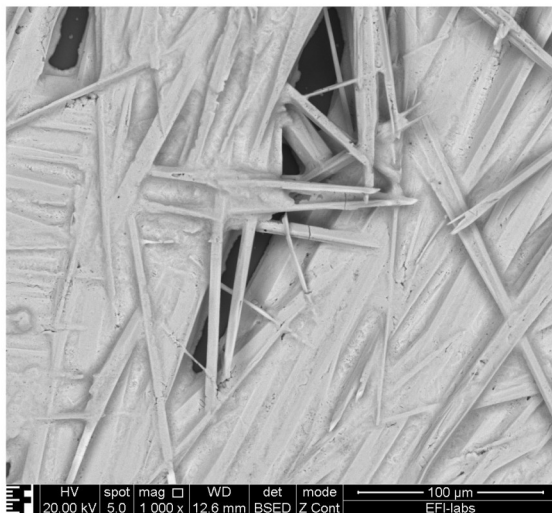


Figure S5. MAPbI₃ crystals after being washed with diethyl-ether, and dried in a vacuum desiccator.

The sample



a.)



b.)

Figure S6. (a.) Sensor with MAPbI₃ body and flat copper electrodes on a 1 m thick, 25 x 25 mm glass plate. (b.) Scanning electron microscope pictures of typical MAPbI₃ layers. For picture parameters, see the lower bar with the black background.

X-ray powder diffraction

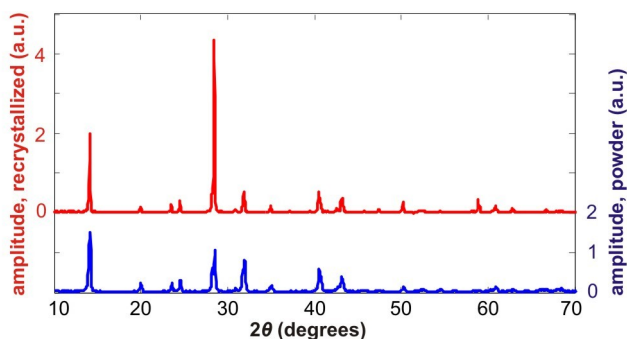


Figure S7. Powder XRD patterns of the studied samples. Blue curve: MAPbI₃ powder, after the full termination of the synthesis, including the 30-min heating at 120°C. Red curve: recrystallized MAPbI₃ prepared from MAPbI₃ dissolved in DMF, while dropping it on a Si plate, drying for 15 min at 40°C, than for 5 min at 120°C. The patterns were recorded by a Philips PW1710/1830 diffractometer with Bragg-Brentano parafocusing system, having monochromatized CuK_α radiation. Counts were recorded with a step size of 0.04°2θ for 1 s in the interval of 10-75°2θ. Both patterns represent tetragonal perovskite structure with I4cm symmetry (unit cell parameters are a=b 8,849 Å, c= 12,642 Å), identical with β-CH₃NH₃PbI₃ sample, determined by single crystal diffraction by Stoumpos et al. (1) and found in the Cambridge Structural Database under the acronym MAPBTI03. In the recrystallized sample the (002) and (004) reflections are more intensive, due to the orientation effect of larger crystals.

(1) Stoumpos, C. C.; Malliakas Ch. D.; Kanatzidis M. G.. *Inorg. Chem.* **2013**, 52, 9019–9038.

Some details of the illumination system

The power values ranged between 2.5 mW and 700 mW, with peak power density values of 0.046 W/cm² and 12.9 W/cm², while the beam had a half-maximum diameter of 2.3 mm. The half-bandwidth for PW (~100 fs) was of ~9 nm, while for CW it was below 1 nm. The adjustment was accomplished by a polarization beam splitter (Foster prism) and a half-wavelength plate (Newport 10RP12-28 in a motorized rotation mount Thorlabs PRM1Z8). Lower power values were achieved by applying neutral density filters (Thorlabs ND05A and ND10A).

Details of the illuminating laser beam

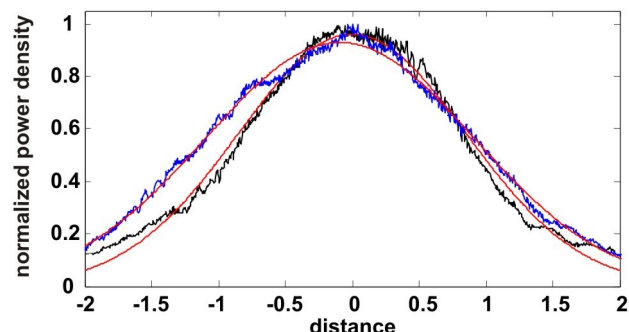


Figure S8.

The illuminating laser beam had a Gaussian profile with standard deviations slightly differing in the horizontal (black curve) and vertical (blue curve) orientations. The profile was independent of the power, and had a small broadening as the wavelength was increased (about 10% between 750 and 900 nm, data not shown). The curves presented above were recorded at 750 nm. The red curves are fitted on the experimental data. The standard deviation averaged on the orientations is 0.93 mm. The averaged peak values for different mean light beam powers are summarized in the following table. Note that the overwhelming majority of the beam power fell on the perovskite layers, which were greater than 5x5 mm.

Beam Power (mW)	2.5	25	100	200	300	400	500	600	700	800
Peak Power Density (W/cm ²)	0.046	0.46	1.8	3.7	5.5	7.4	9.2	11.1	12.9	14.8

Raw voltage trace

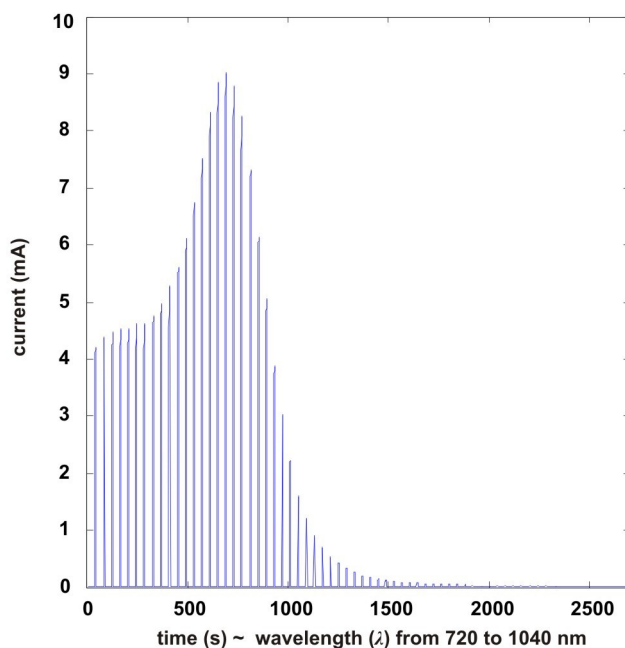


Figure S9.

Representative raw current trace recorded during the photocurrent spectroscopy. Pure MAPbI₃ layer, interdigitated electrodes with 1mm inter-electrode distance, illumination power of 700 mW.

Theoretical

Numerical solution of the mathematical model and the graphical representation of the results were performed by the Matlab software package. For analytical calculations, the Maple package was used.

Computing photocurrent spectra out of the absorption spectrum

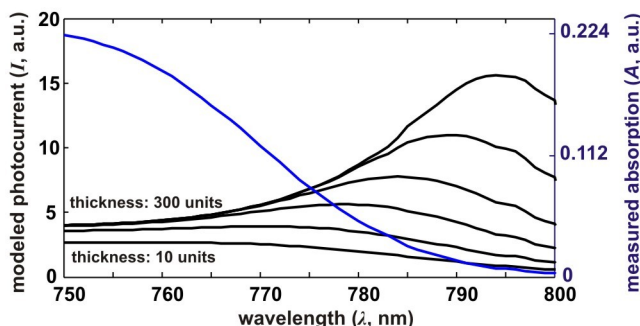


Figure S10.

Photocurrent spectra for samples with different thickness (10, 20, 40, 75, 150, and 300 units) computed using an experimentally recorded optical absorption spectrum (dashed blue line, courtesy of Y. Tian). The absorption spectrum was provided only up to 800 nm. With appropriate γ any z parameters, the model enables to fit the computed photocurrents to the recorded curves.

Simplified Matlab code implementing the core of the 2d photoconductivity model

```
SIG_vol=[];
% conductance of a volume element of the sensor
R_sheet=[];
SIG_sheet=[];
% resistance and conductance of a sheet of the sensor (along the applied voltage)
SIG_total=[];
% total conductance of the sensor (at a given wavelength and incidence angle)

alphaindex=0;
% index for parametrizing the incidence angle

for alpha=[1:-0.01:0].*pi/2
    % incidence angle
    alpha

    alphaindex=alphaindex+1;
    % pi/2 through electrode, 0 perpendicular

    P0=20;
    P01=P0*cos(alpha);
    P02=P0*sin(alpha);
    % photons hitting the sensor
    % (angle modeled by altering the number of photons coming from horizontal and vertical)

    laindex=0;
    % index for parametrizing the wavelength
    for la= [600:1000]
        % wavelength units
        laindex=laindex+1;

        GAMMA=0.55
        PLU=2.5
        ALFA=0.09
        KHI=0.3
        % model parameters

        A(la)=KHI/(PLU+exp(ALFA*(la-770)));
        % assumed sigmoidal absorption, which depends on the wavelength

        for z=1:200
            for x=1:200
                P1(la, z)=P01*exp(-A(la)*z);
                P2(la, x)=P02*exp(-A(la)*x);
                % photons at a certain horizontal (side distance, x) and vertical (depths, z) position

                P(la,x,z)=P1(la, z)+P2(la, x);
                % photons in a volume element at (x,z)
```

```

    % coming from both (horizontal, x and vertical, z) directions

    SIG_vol(la, x,z)=(P(la,x,z)*A(la))^GAMMA;
    % sigma conductivity in a volume element at (x,z),
    % and for a monochromatic illumination with wavelength la
    % (photons x absorbance) on a power
    end %x
end %z

%%%%%%%%%%%%%%%%%%%%%%%%%%%%%%%%%%%%%%%%%%%%%%%%%%%%%%%%%%%%%%%%%%%%%%%%
% Computing the conductivity of a layer at depth z in the sensor
for z=1:200
    % depths from the illuminated z-surface ("column along z")

    R_sheet(la,z)=0;
    for x=1:200
        % side distance from the illuminated x-surface ("sheet along x, at position z")
        R_sheet(la,z)=R_sheet(la,z)+1/SIG_vol(la,x,z);
        % conductances are INVERSE addig
        % volume elements in a sheet are resistors in series, voltage is along the x-coordinate
    end %x

    SIG_sheet(la,z)=1/R_sheet(la,z);
end %z

%%%%%%%%%%%%%%%%%%%%%%%%%%%%%%%%%%%%%%%%%%%%%%%%%%%%%%%%%%%%%%%%%%%%%%%%
% Computing the total conductivity of the sensor

SIG_total(laindex, alphaindex)=0;
% total conductance at a given wavelength and incidence angle

for z=1:200
    % distance (depths) from the illuminated z-surface
    % computation is performed by by adding conductances sheet by sheet
    % each sheet is at a certain depth z
    SIG_total(laindex, alphaindex)=SIG_total(laindex, alphaindex)+SIG_sheet(la,z);
    % conductances are simply adding: sheets are resistors in parallel
end % z
end % la
end % alpha

```

Simplified Matlab code implementing the absorption spectrum reconstruction

```

A=[];
% absorbance
P=[];
% photons at a certain depth z (unity at z=0)
SIG_sheet=[];
% conductance of a sheet at a certain depth z
% note that here a perpendicular illumination is modeled

```

```

SigUptoZ=[];
% conductance of sensors with certain thickness Z
Root1=[];
Root2=[];
% segments of the recomputed absorbance

LIM1=700
LIM2=920
% wavelength unit limits
ZMAX=500
% maximal thickness units

PLU=2.5
ALFA=0.09
KHI=0.3
GAMMA=0.55
% model parameters

for la= LIM1:LIM2
    % wavelength units
    A(la)=KHI/(PLU+exp(ALFA*(la-770)));
    % expression of the sigmoid absorbance
    for z=1:ZMAX
        % depth measured from the illuminated surface
        P(la,z)=1*exp(-A(la)*z);
        % photons at a certain depths (illumination intensity=1)
        SIG_sheet(la, z)=(P(la,z)*A(la))^GAMMA;
        % sigma conductance in a SHEET at depth z:
        % photons times absorbance at a GAMMA power
    end % z
end % la

%%%%%%%% As follows, we recompute A from SIG_sheet %%%%%%%%%%
for la=LIM1:LIM2
    % wavelength units
    for z=1:ZMAX
        % depth z measured from the illuminated surface, perpendicular arrangement
        derivz(la, z)=SIG_sheet(la, z);
        % the derivative of the photocurrent with respect to the depth z
        % this equals the photocurrent contribution from the sheet at z
        ypsilon(la, z)=derivz(la, z)^(1/GAMMA);
        % this variable corresponds to Y(Z) in the paper
    end %z
end %la

%%%%%%%%%
for z=[20 100 ZMAX]
    % depth measured from the illuminated surface
    for la=720:920
        % wavelength units

```

```

fun2=@(AA) ypsilon(la, z)- AA.*exp(-AA.*z)
% anonymous Matlab function
% A*exp(-Az) is a peak shape function, see at the end of the software
% here we implement the solving of Y(Z)-AA*exp(-AA*z)=0 for AA
% AA corresponds to the recomputed absorption

ApproxParam1=0.001;
% parameter defining where to start the approximation
Root1(la, z)=fzero(fun2, ApproxParam1);
% fzero finds a root starting from the second argument
% we have two roots; looking for the close-to-zero root here

if z==20 ApproxParam2=0.1; end
if z==100 ApproxParam2=0.1; end
if z==ZMAX ApproxParam2=0.065; end
% parameter defining where to start the approximation

Root2(la, z)=fzero(fun2, ApproxParam2);
% we have two roots; looking for the far-from-zero root here
end % la
end % z

%%%%%%%%%%%%%%%%%%%%%%%%%%%%%%%%%%%%%%%%%%%%%%%%%%%%%%%%%%%%%%%%%%%%%%%%

figure('Position',[10 10 1000 500],'Color','w');
plot(A(:), 'color', [0.3 0.3 0.3], 'linewidth', 8, 'linestyle', '-'); hold on;
for z=[20 100 ZMAX]
    if z==20 asym='+'; end;
    if z==100 asym='>'; end;
    if z==ZMAX asym='o';end;
    if z==20 c1=[0 0.7 0]; c2=[1 0.1 0.5]; end
    if z==100 c1=[0 0 1]; c2=[1 0 0]; end
    if z==ZMAX c1=[0 1 1]; c2=[1 0.5 0]; end
    plot(Root1(:,z), 'color', c1, 'linestyle', asym); hold on;
    plot(Root2(:,z), 'color', c2, 'linestyle', asym); hold on;
end
xlim([720, 920])
ylim([0 0.155])

set(gca, 'FontSize', 16)

```

Simplified Matlab code of the microscopic reaction-diffusion model

```

n=[];
% charge carrier density
SIG=[];
% conductance of a sensor layer
SigUptoZ=[];
% conductance of whole sensors with different thickness
TMAX=2001;

```

```

% iteration number (scaled time)
ZMAX=500;
% maximal (scaled) sensor thickness investigated
LLIM1=680;
LLIM2=920;
% higher and lower wavelength limits
P0=0.1
% illumination intensity

TAUM=0.1;
% recombination constant
D=1;
% charge carrier diffusion constant
dz=1;
% space scaling parameter
dt=0.01;
% time scaling parameter

NP=[1 30:10:ZMAX];
% position of the layers with intense recombination
% (several ones used, e.g. NP=[] for the plain model, NP=[1] for surface
recombination)
n(LLIM1:LLIM2, 1:ZMAX, 1:TMAX)=0;
% initial condition for charge carrier density

for t=1:TMAX
    % time t
    t
    for la=LLIM1:LLIM2
        % wavelength la
        % we assume a monochromatic illumination
        A(la)=0.1/(1+exp(0.1*(la-770)));
        % assumed sigmoid absorbance, which depends on the wavelength
        for z=1:ZMAX
            % depth z measured from the illuminated surface
            P(la,z)=P0*exp(-A(la)*z);
            % photons at a certain depths z, and for an illumination with a
wavelength la
            n_generate(la,z)=P(la,z)*A(la);
            % photons generated by an illumination with wavelength la, at
depth z

```

```

    % note that n_generate does not depend on time in this model
end %z

for z=2:ZMAX-1
    n(la, z,t+1)=n(la, z,t)
    +dt*(D*(n(la, z+1,t)-2*n(la, z,t)+n(la, z-1,t))/(dz*dz)
    -n(la, z,t)*TAUM+n_generate(la,z));
    % implemtation of the model; n represents the charge carrier den-
density
    % diffusion term (monochromatic illumination assumed!
    % separate for each la wavelength)
    % recombination term, (photo)generation term
end %z

n(la, 1, t+1)= (n(la, 1,t)+ dt*(D*(n(la, 2,t)-n(la, 1,t))/(dz*dz)
-n(la, 1,t)*TAUM+n_generate(la,1) ) );
n(la, ZMAX, t+1)=(n(la, ZMAX,t)+ dt*(D*(-n(la, ZMAX,t)+n(la, ZMAX-
1,t))/(dz*dz)
-n(la, ZMAX,t)*TAUM+n_generate(la,ZMAX) ));
    % boundary conditions at the surfaces

if ~isempty(NP)
    for ii=1:length(NP)
        n(la, NP(ii),t+1)=0;
        % implementation of the recombination sites
    end %NP
end %if

end %la
end %
%%%%%%%%%%%%%%
%%%%%%%%%%
SIG=n;
% conductivity (of the layer in depth z, and for an illumination with a
wavelength la)
% assumed to be proportional to the charge carrier density n

for t=1:TMAX
    % time t
    t
    for la=LLIM1:LLIM2
        % wavelength la

```


Varying the photocurrent spectrum by placing recombination sites to certain depth in the sample

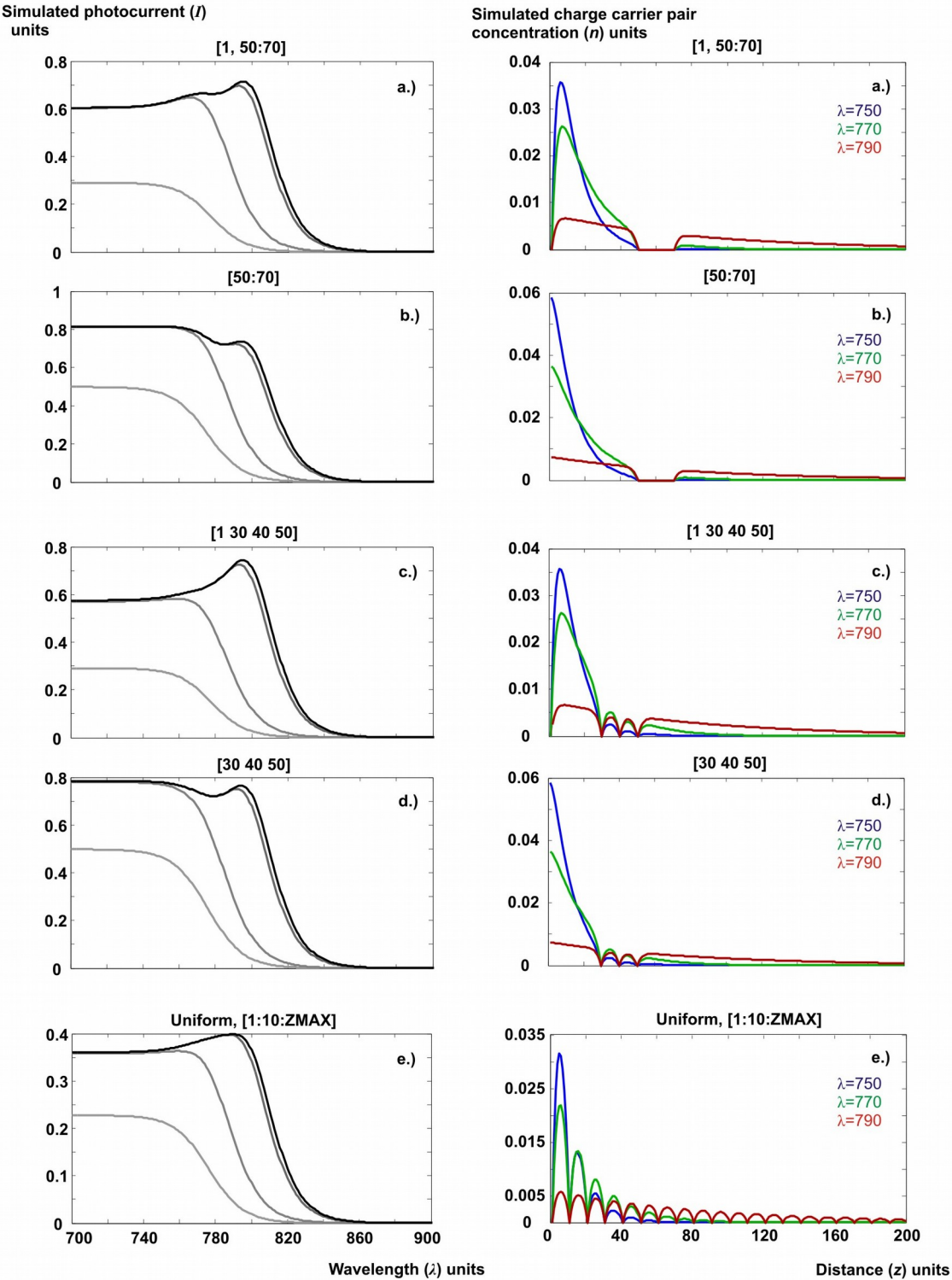


Figure S11. Simulated photocurrent and charge carrier pair concentrations for recombination sites at various locations. The parameters, except the location of the recombination sites, are the same as for Fig. 8, while the latter are marked on the left figures. On the right figures, blue, green and red curves represent simulations with $\lambda=750$, $\lambda=770$, and $\lambda=790$ wavelength units.

Density of charge carrier pairs in modeled samples with different recombination sites

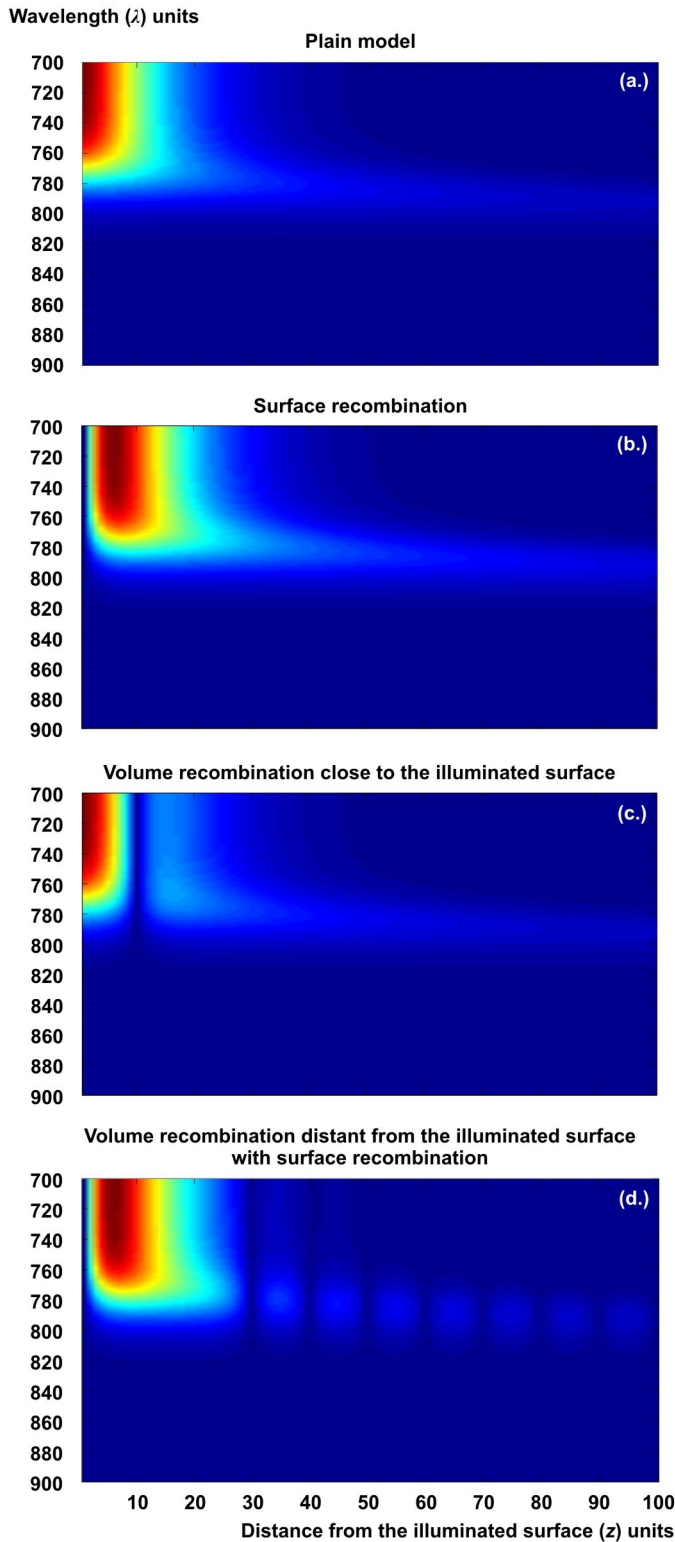


Fig. S12.

Simulated density n of charge carrier pairs, resulting from the reaction-diffusion model. The density of charge carrier pairs is a function of the depth measured from the illuminated surface ($z=0$) and that of the monochro-

matic wavelength. The light penetrates in the sample from left, where $z=0$. Blue corresponds to zero, while dark red to the highest values. (a.) No recombination sites (where $n=0$) are present. (b.) Recombination site placed at the illuminated surface. (c.) Recombination site in the volume of the sensor, but close to the illuminated surface. (d.) Besides a surface recombination site, a series of volume recombination sites, farther from the illuminated surface, are also present.

Dimensionless form of the microscopic reaction-diffusion model

Let us to rescale the time, distance and concentration as follows:

$$t' = t/T$$

$$z' = z/L$$

$$n' = n/N$$

Inserting the above in the reaction-diffusion equation describing the spatio-temporal dynamics of the charge carriers, we have

$$\frac{N}{T} \frac{\partial n'}{\partial t} = D \frac{N}{L^2} \frac{\partial n'}{\partial z'^2} + P(z)A + \frac{1}{\tau} n'$$

Rearranging this follows

$$\frac{\partial n'}{\partial t} = D \frac{T}{L^2} \frac{\partial n'}{\partial z'^2} + \frac{T}{N} P(z)A + \frac{T}{\tau} n'$$

By setting the length scale (L) the time scale (T) and the concentration scale (N), we can have

$$D \frac{T}{L^2} = 1$$

$$\frac{T}{N} A = 1$$

$$\frac{T}{\tau} = 1$$

Note that L sets the value of diffusion length, while T the value of the decay time. Therefore, with this choice, the equation simplifies to

$$\frac{\partial n'}{\partial t} = \frac{\partial n'}{\partial z'^2} + P(z)A + n'$$

We have to rescale, in a similar way, the initial and boundary conditions as well.

Further photocurrent-based methods applied in semiconductor research

A broad variety of methods relying on light-induced currents are applied for semiconductor research. The most important ones are the modulated^a, the Fourier-transform based^b, the differential^c and the time-resolved^d photocurrent spectroscopy, as well as the constant photocurrent method^{e,f}. In this paper we just apply the simplest, time-domain and DC version of these approaches.

(a) Erhard N.; Holleitner, A. Semiconductor nanowires studied by photocurrent spectroscopy, in: *Semiconductor Nanowires: Materials, Synthesis, Characterization and Applications* 365-393, **2015**, eds.: Arbiol, J.; Xiong, Q. Woodhead Publishing.

(b) Tober, R. L.; Li, W. Q.; Bhattacharya, P. K. Differential photocurrent spectroscopy: A novel technique for semiconductor characterization, *J. Appl. Phys.* **1992**, 71, 3506-3508.

(c) Hamadani, B. H.; Roller, J.; Kounavis, P.; Zhitenev, N. B.; Gundlach, D. Modulated photocurrent spectroscopy of CdTe/CdS solar cells - equivalent circuit analysis, *Sol. Energ. Mat. Sol. Cells* **2013**, 116, 126-134.

(d) Holovsky, J. Fourier Transform Photocurrent Spectroscopy on Non-Crystalline Semiconductors, in: *Fourier Transforms - New Analytical Approaches and FTIR Strategies*, www.intechopen.com/books/fourier-transforms-new-analytical-approaches-and-ftir-strategies (accessed 12.01.2017)

(e) Vanecek, M; Kocka, J; Poruba, A; Ferfar, A; Direct measurement of the deep defect density in thin amorphous silicon films with the "absolute" constant photocurrent method, *J. Appl. Phys.* **1995**, 78, 6203-6210

(f) Vanecek, M; Kocka, M; Stuchlik, J; Triska, A; Direct measurement of the gap states and band tail absorption by constant photocurrent method in amorphous silicon, *Solid State Commun.* **1981**, 39, 1199-1202